

# Performing tip-enhanced Raman spectroscopy in liquids

Thomas Schmid,<sup>†</sup> Boon-Siang Yeo,<sup>†</sup> Grace Leong, Johannes Stadler and Renato Zenobi\*

Many outstanding questions in biology and medicine require analytical tools that provide imaging and chemical information with high spatial resolution. Tip-enhanced Raman spectroscopy (TERS) has been shown to allow both topographic and label-free chemical information to be obtained with a lateral resolution of approximately 20–50 nm, but has been performed only in air or ultrahigh vacuum until now. Since most biological samples such as cells and tissues can only be studied in their active state if they are kept in aqueous buffers, TERS in liquids would be a crucial step towards nanoscale chemical analysis of living biological entities. For the first time, we introduce TERS experiments that have been performed with both the tip and sample completely immersed in water. We demonstrate that SiO<sub>x</sub>/Ag-coated AFM tips provide enhancement factors of > 10<sup>4</sup> with visible light irradiation and are robust enough to be used in water. Furthermore, the tips have been protected from contaminants by adsorbing a self-assembled monolayer (SAM) of ethanethiolate on their Ag surfaces. The protection layer caused the enhancement to drop by a factor of approximately 5, but successfully prevented the adsorption of analyte molecules, carbon, and other contamination to the tip. Furthermore, our experiments have shown that the formation of carbonaceous contamination by laser irradiation on the tip is dramatically slowed down when TERS experiments are performed in water. Finally, a proof-of-principle study on SAMs of thiophenolate on Au surfaces demonstrates the feasibility of performing TERS in liquids. Copyright © 2009 John Wiley & Sons, Ltd.

**Keywords:** tip-enhanced Raman spectroscopy (TERS); liquids; nanoscale chemical analysis; thiophenol self-assembled monolayer (SAM)

## Introduction

Many outstanding questions in biology and medicine regarding cell growth and transformation, cell–cell signaling, adhesion, ion channels, activity of membrane-bound enzymes etc. require analytical tools that provide imaging and chemical information with high spatial resolution. For example, the determination of protein–protein distances, colocalization of membrane proteins, or the distribution of lipid rafts in membranes can only be performed with microscopy techniques that provide resolution in the nanometer regime, well below the optical diffraction limit.<sup>[1–3]</sup>

Tip-enhanced Raman spectroscopy (TERS) has been shown to allow both topographic and label-free chemical/molecular information to be obtained with a resolution of 20–50 nm laterally.<sup>[4–7]</sup> After the first demonstrations of the TERS effect in 2000,<sup>[8–10]</sup> research in this field has followed a two-pronged approach. On one hand, the TERS effect with a focus on its enhancement has been studied. Here, mainly highly Raman active chemical species, such as resonantly excited dye molecules, have been used as analyte molecules.<sup>[7,8,10–14]</sup> This approach has led to first reports of single-molecule sensitivity in TERS.<sup>[15–18]</sup> On the other hand, a few groups have focused on applications of TERS to topics in chemistry, materials science, and biology.<sup>[4]</sup> A classical example would be the TERS imaging of single-walled carbon nanotubes, which allows, for example, the detection of local variations of the tube diameter.<sup>[5,19–24]</sup> During the last few years, studies on biological systems using TERS have begun to appear. TER spectra of biomolecules with reasonable signal-to-noise ratios are more difficult to obtain due to their generally lower Raman scattering cross sections as compared to dye molecules or carbon nanotubes. The applications range from small biomolecules, such

as adenine,<sup>[25,26]</sup> over the biopolymers alginate,<sup>[27,28]</sup> cytochrome c,<sup>[29]</sup> and RNA,<sup>[30]</sup> to living bacterial cells.<sup>[31,32]</sup> However, all these TERS measurements have been performed in air. Even bacterial cells have been investigated in air. For this study, skin bacteria of the species *Staphylococcus epidermidis* have been chosen as a sample organism, because they are known to be viable even in air. This is not true for most other biological cells and tissues, which can only be studied in the living state if they are kept in an aqueous buffer solution. Also, isolated biological membranes or supported lipid bilayers – a hot topic in materials research – can only be studied in an aqueous environment, because they usually collapse in the dry state.

Recent studies have demonstrated that near-field fluorescence microscopies are able to image biological entities in water with high spatial resolution and chemical contrast. Aperture scanning near-field optical microscopy (a-SNOM) of fluorescently labeled interleukin (IL) 2 and IL 15 alpha subunits in the membrane of human T-lymphoma cells has shown the potential of chemical high-resolution imaging of biological systems.<sup>[1]</sup> Whereas confocal fluorescence images seemed to speak for a colocalization of IL2 and IL15, high-resolution SNOM images contradicted this postulate by revealing isolated monomers as well as clusters of different sizes.

\* Correspondence to: Renato Zenobi, Department of Chemistry and Applied Biosciences, ETH Zurich, Wolfgang-Pauli-Strasse 10, 8093 Zurich, Switzerland. E-mail: zenobi@org.chem.ethz.ch

† These authors contributed equally to this work.

Department of Chemistry and Applied Biosciences, ETH Zurich, Wolfgang-Pauli-Strasse 10, 8093 Zurich, Switzerland

This approach opens up the possibility to study distances and colocalization of membrane proteins and lipid rafts in order to gain better insight into the importance of lipid rafts in membrane-protein activities. Our group has demonstrated the potential of a-SNOM combined with Raman spectroscopy in the study of liquid–liquid interfaces, taking advantage of the high resolution of a-SNOM in the  $z$  (tip) direction.<sup>[33,34]</sup> However, aperture glass fiber probes provide only low irradiance at the sample because of their limited optical transmission, and restrict the lateral resolution to approximately 100 nm; i.e. the simultaneous optical and topographic imaging with high speed and high spatial resolution is virtually impossible.<sup>[2]</sup> However, this is exactly what would be required to gain valuable information on correlations between protein distribution and structural properties of the cell surface. In order to overcome these drawbacks, antenna-based apertureless near-field fluorescence imaging has been proposed and demonstrated successfully in the imaging of single  $\text{Ca}^{2+}$  transmembrane proteins in red blood cell membranes.<sup>[2]</sup> The main drawback of fluorescence approaches is the need for labeling, which always represents an interference with the biological system under study. Thus, errors resulting from changed behavior of the labeled molecules, unspecific staining, or toxic effects often cannot be totally ruled out. Additionally, labeling requires knowledge on the presence of a certain analyte and the availability of suitable fluorescent labels or strategies for *in situ* staining. Also the number of analyte molecules that can be simultaneously imaged is limited due to practical restrictions. Only label-free techniques, which provide spectroscopic fingerprints at each pixel, give us the chance to discover previously unknown molecules and to map out the distribution of large numbers of different analytes at the same time.

This paper is the first report on TERS experiments performed in water. The analyte in this proof-of-principle study is a self-assembled monolayer (SAM) of thiophenolate (PhS) on a Au surface. Its vibrational signature has been successfully detected, and enhancement factors of approximately  $5 \times 10^3$  have been determined. Furthermore, strategies for production of robust TERS tips are presented that provide reasonable enhancement in water and are protected from contaminants.

## Experimental

### Experimental setup

The setup for TERS used in this study is a home-built combination of an inverted confocal laser-scanning microscope (CLSM, FluoView FV500, Olympus, Melville, NY), a Raman spectrograph (Holospec  $f/1.8i$ , Kaiser Optical Systems, Ann Arbor, MI), an atomic force microscope (AFM, Explorer, Veeco Instruments, Santa Barbara, CA, controlled by SPMLab software, Veeco Instruments), and a piezo-driven stage for scanning the sample (P-500 series PZT Stage, Physik Instrumente, Waldbronn, Germany). The apparatus is described in more detail in Ref. [35]. For excitation, a diode-pumped solid-state laser with a wavelength of 532 nm and a tunable output power of  $\leq 100$  mW was coupled fiber-optically into the system. The laser beam was focused using a  $60\times/\text{N.A.} = 1.4$  oil immersion objective through a transparent glass substrate (see below) onto the sample layer and the AFM tip. Raman signals were collected through the same objective, passed through a beam splitter and guided via fiber optics into the spectrograph. Typical laser powers at the sample were in the range of 2–100  $\mu\text{W}$ . Similar values have been applied previously in TERS experiments by our group.<sup>[36]</sup> The AFM is equipped for scanning in liquid

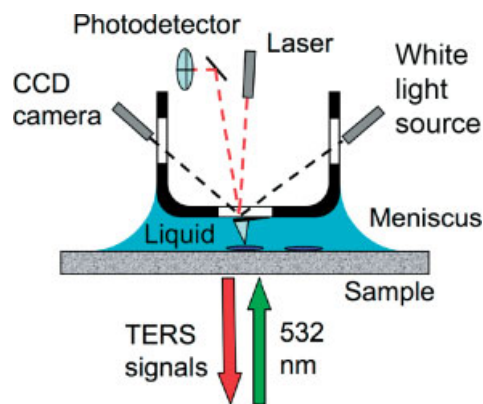


Figure 1. Schematic diagram of the TERS setup in aqueous conditions.

without the need of a closed sample cell. The tip is mounted below a Teflon plate with a window for the AFM feedback laser and observation of the sample from the top using a CCD camera (Fig. 1). Sample and tip are immersed in a droplet of water in such a way that a meniscus is formed from the sample substrate to the Teflon plate and water fills the entire gap. This ‘open cell’ configuration allows the scanning of the sample in liquid with a fixed alignment between laser beam and tip, an important prerequisite for TERS measurements on different sample spots under constant excitation conditions.

### Preparation of TERS tips

TERS tips were prepared by vapor-coating of commercially available contact-mode silicon nitride AFM tips (RC800PSA, Olympus, Tokyo, Japan) in a vapor-coating chamber (MED 020, Bal-Tec, Balzers, Liechtenstein) equipped with a quartz crystal microbalance (QCM, QSG 060, Bal-Tec, Balzers, Liechtenstein) for monitoring of the film thickness. The tips were mounted 15 cm above the evaporation source in the chamber. A two-layer coating was employed, as described in Ref. [36]. For the first layer,  $\text{AlF}_3$  (99%, Aldrich) or silicon monoxide (99.99%, Aldrich) was sublimated by resistive heating, and a 20-nm-thick layer was coated onto the tips at a rate of  $0.1 \text{ nm s}^{-1}$ . Subsequently, a 30-nm layer of Ag (99.99%, Bal-Tec) was coated on top at a rate of  $0.05 \text{ nm s}^{-1}$ . These Au films were sufficiently optically transparent to allow illumination and collection of scattered light through the films, from below.

Recent studies by our group have demonstrated that TERS tips with high enhancement factors for excitation in the blue to green spectral region can be manufactured by this two-layer coating method.<sup>[36,37]</sup> The contact of Ag to higher refractive index materials usually causes a red shift of the surface plasmon resonance frequency. This effect is reduced when an Ag layer is in contact with low refractive index materials. Thus, the surface plasmon resonance wavelength can be tuned to better coincide with the laser wavelength, which results in a stronger enhancement of the electromagnetic field. The low refractive index materials used by our group for this purpose are silicon oxide, which forms layers of  $\text{SiO}_x$  (with  $x = 1 \dots 2$ ) after vapor coating, with refractive indices ranging from  $n = 1.5$  ( $x = 2$ ) to  $n = 2.05$  ( $x = 1$ ), and  $\text{AlF}_3$  with  $n = 1.4$ .

### Protection of TERS tips

In order to protect the Ag surface of the TERS tips from being contaminated with carbon, analyte molecules, and other

contaminants, they were coated with a SAM of ethanethiolate (EtS). TERS tips were immersed in a  $10^{-3}$  M solution of ethanethiol (EtSH, 99 + %, Acros) in ethanol for 5 min to allow a SAM of EtS to form on the Ag surface. The tips were rinsed with ethanol and air-dried.

## Samples

### Chemicals

The samples under investigation in this proof-of-principle study were thin films or SAMs of brilliant cresyl blue dye (BCB, Fluka) and thiophenol (PhSH, 99 + %, Acros), respectively. Deionized water was drawn from a NANOpure Diamond (Barnstead) apparatus.

### Sample substrates

All samples investigated in this study were coated onto glass cover slips ( $24 \times 24$  mm<sup>2</sup>, Paul Marienfeld GmbH & Co. KG, Lauda-Königshofen, Germany). Before use, the glass slides were cleaned by immersion in piranha solution ( $\text{H}_2\text{SO}_4 + \text{H}_2\text{O}_2$ , 3 : 1) for at least 30 min. They were rinsed with water and methanol and dried under a stream of  $\text{N}_2$  gas. SERS substrates were prepared by vapor-coating 6 nm of Ag (99.99%, Bal-Tec) onto clean glass slides at a rate of  $0.05$  nm  $\text{s}^{-1}$ . Au films as substrates for PhS SAMs were made by vapor-coating clean glass slides with 2 nm of a Cr adhesive layer (99.98%, Bal-Tec), followed by 6 nm of Au (99.99%, Bal-Tec), both at a rate of  $0.05$  nm  $\text{s}^{-1}$ .

### Sample preparation

Thin films of BCB were prepared by spin-coating 10  $\mu\text{l}$  of a  $10^{-4}$  M BCB solution in methanol onto clean glass slides. PhS SAMs were made by immersion of Au-coated glass slides in  $10^{-3}$  M PhSH solution in ethanol for 5 min. Unbound or weakly bound molecules were rinsed off with copious amounts of ethanol. Subsequently, the slides were dried under a  $\text{N}_2$  gas flow.

## Data processing

No background correction or smoothening of the spectra was performed. The data points were processed using Igor Pro Version 4.08 Carbon (Wavemetrics). For presentation in this paper, some spectra have been baseline-shifted for better visibility of the individual spectra.

## Results and Discussion

### Can a TERS tip stay intact in water?

Since Ag coating of the tip is essential for TERS enhancement, a critical question is its stability in a liquid environment. A batch of 10 tips was prepared and half of the TERS tips made were randomly selected. These were soaked in water for 1 h and then air-dried. One hour was the typical time a tip was used in the TERS measurements presented here. Scanning electron microscopy (SEM) images were taken of these tips, with the unsoaked ones as control. This procedure was followed for both  $\text{AlF}_3/\text{Ag}$ -coated and  $\text{SiO}_x/\text{Ag}$ -coated tips (see Experimental section).

When performing TERS in air with laser excitation in the blue to green spectral range,  $\text{AlF}_3$  is the better choice of a dielectric support material as compared to  $\text{SiO}_x$ , because  $\text{AlF}_3$  has a lower evaporation temperature than  $\text{SiO}$ , a lower refractive index of  $n = 1.4$ , and a

consistent stoichiometry resulting in a well-defined  $n$ .<sup>[36]</sup> Excitation in the blue to green range was chosen because of two reasons: (1) high enhancement has been obtained in this range with Ag-coated tips, and (2) the AFM uses a 650-nm diode laser for the measurement of the cantilever deflection. Thus, if a red laser were to be used, e.g. a He–Ne laser with  $\lambda = 632.8$  nm, the emission of the AFM laser diode would overwhelm the Raman bands in the fingerprint range of organic molecules. Additionally, a red laser could cause cross-talk with the AFM feedback. Unfortunately,  $\text{AlF}_3/\text{Ag}$ -coated tips were found to be unsuitable for performing TERS in water. Figure 2(a) is a typical SEM image of an  $\text{AlF}_3/\text{Ag}$ -coated AFM tip. In Fig. 2(b) the effect of soaking such a tip in water can be seen. The action of water, or possibly the combined effects of soaking and drying, results in the coating layer peeling off. In the case shown, the Ag particles have been lost on three sides of the pyramidal tip, including the tip apex. Since the presence of an enhancing silver particle at the tip apex is crucial for a TERS experiment,  $\text{AlF}_3/\text{Ag}$ -coated AFM tips cannot be used in TERS measurements in water or aqueous buffers.

In our experience,  $\text{SiO}_x/\text{Ag}$ -coated AFM tips also yield reasonably high enhancement with laser excitation in the blue to green spectral range in air,<sup>[36]</sup> and were found to be suitable for experiments in liquids. On many SEM images, no significant change in morphology of the coating layer was observed after soaking the tips in water. On some images, the loss of only a small number of isolated Ag particles on the side walls of the pyramidal AFM tips was observed, as highlighted in Fig. 2(d) by the dashed circle. It should be pointed out that even in these cases, the particle at the tip end, which would be mainly responsible for the TERS enhancement, remained unchanged.

It can also be noted in Fig. 2(d) that the Ag nanoparticles were detached from the  $\text{SiO}_x/\text{Ag}$ -coated tip individually. This indicates that they are adsorbed on the tip separately, and not in the form of a continuous film. This information is not available from SEM images of TERS tips taken directly after coating (Fig. 2(a) and (c)). There, the SEM images do not clearly indicate whether the densely packed Ag nanoparticles are in the form of a continuous film or individually attached. This information will be useful for future numerical simulations of Ag-coated dielectric tips.

### TERS of PhS on Au surfaces in water

The results in the previous section have demonstrated the robustness of  $\text{SiO}_x/\text{Ag}$ -coated AFM tips in water. From previous TERS experiments performed in air, we know that they are able to give reasonable enhancement with 532-nm excitation. Thus, a first attempt for a proof-of-principle experiment for TERS in liquids was made. One of our concerns was whether the desorption of analyte molecules from the surface of the substrate and subsequent (undesired) adsorption of the analyte to the tip or at least diffusion and re-orientation of molecules on the substrate would be a problem in a liquid TERS experiment. This could cause fluctuations of TERS signals, complicate data interpretation, and eventually lead to irreversible contamination of the tip. Therefore, we used analyte molecules that are covalently linked to the substrate in a well-defined manner and whose Raman spectra are well understood: a SAM of PhS on a gold surface.<sup>[38,39]</sup>

As described in the Experimental section, sample and tip were immersed into a droplet of water forming an 'open' liquid cell and the tip was made to approach the sample (contact-mode AFM feedback). The laser spot was focused onto the tip apex, and the spectrum (a) in Fig. 3 was collected within 10 s acquisition time.

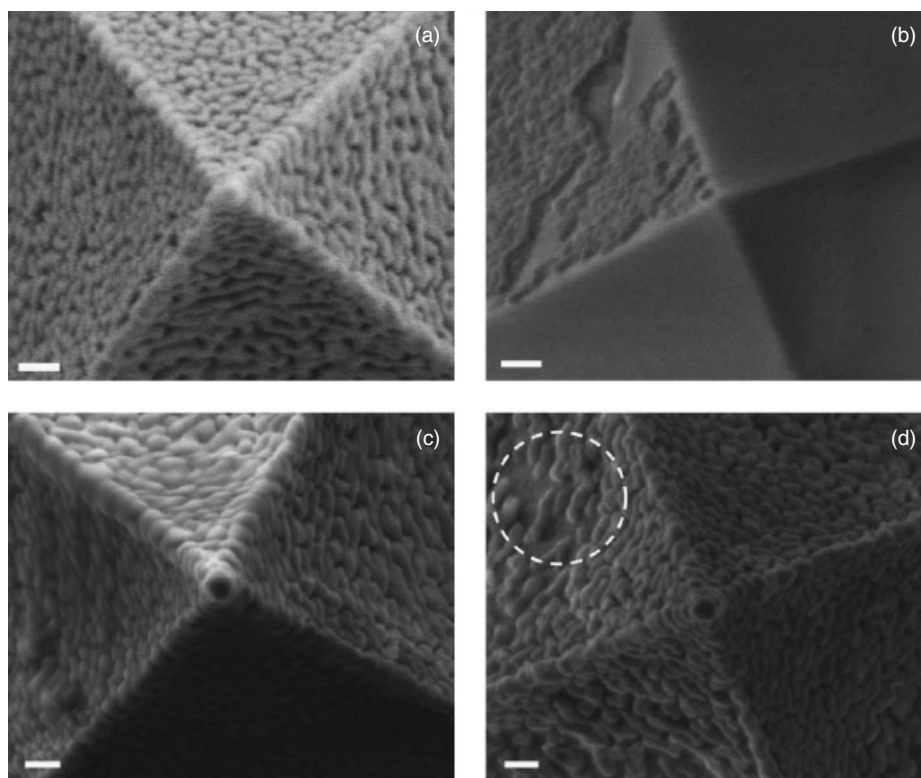


**Figure 2.** SEM images of TERS tips (tip apex in the center of each image):  $\text{AlF}_3/\text{Ag}$ -coated tip (a) before and (b) after soaking in water for 1 h, and  $\text{SiO}_x/\text{Ag}$ -coated tip (c) before and (d) after soaking in water for 1 h. The scale bars represent 100 nm. The dotted circle highlights the detachment of a few individual Ag particles under the action of water from the side wall of the tip (see text).

The vibrational features that can be assigned to PhS are labeled in the spectrum.<sup>[39]</sup> Then, the tip was retracted from the surface, far enough to be outside the laser focus. Under the same conditions (10 s acquisition time), a far-field spectrum was recorded (spectrum (c) in Fig. 3). In order to ensure that the PhS signals in the TER spectrum originated from analyte molecules on the sample substrate and to estimate the extent of tip contamination, a control experiment was performed: the same tip was brought into contact with a clean Au surface. The laser was focused onto the tip apex, and spectrum (b) in Fig. 3 was recorded within 10 s.

In the TER spectrum (Fig. 3(a)), the four most prominent bands of PhS at  $1000$ ,  $1023$ ,  $1073$ , and  $1576\text{ cm}^{-1}$  can be clearly identified. With the tip retracted (far-field spectrum, Fig. 3(c)), these cannot be distinguished from the noise, which is an indication of a strong enhancement effect by the tip. The control experiment (Fig. 3(b)) clearly shows two effects: (1) analyte molecules desorb from the Au surface and bind to the tip and (2) contamination of the tip with carbonaceous material has a significant influence. Effect (1) can be deduced from the fact that also in the control experiment PhS signals are clearly detectable, with similar signal intensities as in spectrum (a). This effect was observed in every experiment, regardless of tip–sample contact time and laser power. We conclude that the effect is intrinsic to the system, and we rationalized it as being due to the higher surface free energy of the rough Ag tip as compared to the smooth Au surface. This phenomenon has also been observed in previous TERS studies performed in air.<sup>[40,41]</sup>

Additionally, strong Raman scattering was detected in the control experiment in the range of approximately  $1100$ – $1700\text{ cm}^{-1}$  with mainly two broad bands centered at approximately  $1360$  and  $1590\text{ cm}^{-1}$ . These are the D and G band of amorphous carbon

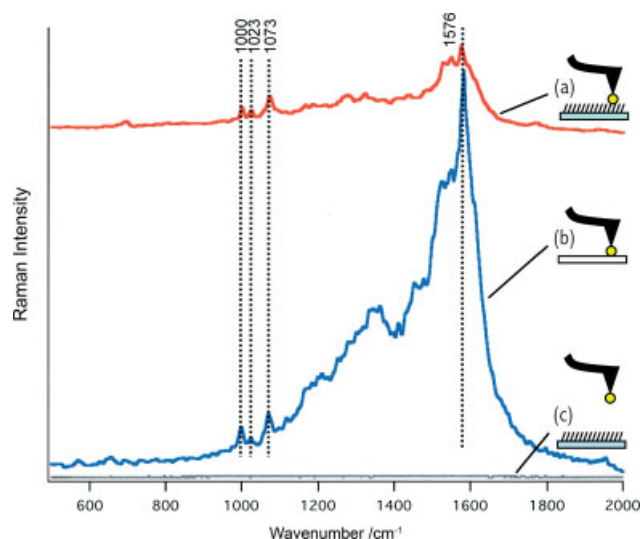


**Figure 3.** TERS measurements of a SAM of PhS on a Au surface collected in water: (a) TER spectrum obtained with a  $\text{SiO}_x/\text{Ag}$ -coated tip in contact with the sample, (b) control measurement performed after the TERS measurement with the same tip in contact with a clean Au substrate, and (c) far-field spectrum of the PhS SAM on Au. The collection time for each measurement was 10 s.

and are typical contamination bands known in TERS experiments (effect (2)).<sup>[42,43]</sup> In all experiments performed during this study, the carbon signals got stronger with longer laser irradiation of the tip. This is clearly visible in Fig. 3, where the TER spectrum recorded first (spectrum (a)) shows a relatively weak contribution from car-

boneaceous material, whereas spectrum (b), which was recorded subsequently, contains a more intense carbon spectrum. Thus, we can conclude that the carbonaceous contaminants were mostly generated during the experiment under the influence of laser irradiation. Precursors for carbon might already have been present on the tip surface directly after the coating process, adsorbed from the atmosphere or the liquid phase, or simply consisted of analyte molecules that have photodissociated into carbonaceous products. It should be mentioned that no carbon signals were detected when the Au substrate was measured without a tip in contact. This is not necessarily due to the absence of carbon on the Au surface, but most likely due to the lack of SERS enhancement of such substrates with 532-nm excitation.

Figure 3 demonstrates the feasibility for collection of TERS spectra in liquid environment, but the two effects that arise from binding of analyte molecules and/or other contaminants to the tip surface hamper the realization of TERS imaging in liquids. If the tip was contaminated by the analyte in an imaging experiment, the same spectrum would be observed on every pixel even in the case of highly heterogeneous samples. The strong carbon contamination signals overwhelm signals of analytes in a relatively wide spectral range, making it even difficult in this example to identify the relatively strong PhS band at  $1576\text{ cm}^{-1}$ . The extent of analyte desorption from the substrate and binding to the tip surely depends on the sample under investigation, but we expect this effect to be facilitated by the liquid environment. Thus, we searched for a strategy to protect the tip from contaminations, which is described in the following section.

### Protection of TERS tips with a SAM of EtS

Tip protection should be able to prevent the unwanted binding of molecules to the tip during the experiment or even remove/replace contaminations. We chose a SAM of EtS as the protection layer for several reasons. First, EtS is known to build a well-defined, dense, chemisorbed SAM on Ag surfaces and thus can replace contaminants. Second, EtS has a length of only  $\sim 4.5\text{ \AA}$ , far below the extent of the enhanced field, which is known to extend  $10\text{--}30\text{ nm}$  from the tip into the surrounding medium.<sup>[44,45]</sup> Finite-element simulations predict an  $e^{-z/R}$  dependence of the field enhancement of a tip with radius  $R$  over the distance  $z$  from its surface.<sup>[46]</sup> The extension of the enhanced field is on the order of the tip radius and can thus be even smaller than  $10\text{ nm}$  for very sharp tips. Even in such cases, the enhanced field would be an order of magnitude larger than the EtS coating. Hence, the field enhancement afforded by the tip should still be accessible by the sample surface. Third, EtS has well-known vibrational features<sup>[47]</sup> that do not overlap with those of PhS, which is the analyte molecule in this proof-of-principle study. In general, we expect spectral interference to be a minor problem for most analyte molecules, because with our typical conditions for a TERS experiment (low laser power, relatively short measurement times), only one sharp band at  $633\text{ cm}^{-1}$  was detectable that can be assigned to the C–S stretching vibration of EtS.

In a first step, the effects of tip protection in air and water were studied systematically using Ag-coated glass slides and performing SERS measurements. Subsequently, the results of the SERS experiment were extrapolated to TERS with Ag-coated tips. This strategy of studying enhancement effects first systematically in SERS experiments, where a higher number of measurements can be performed more easily and then confirming the validity of the results also in a TERS setting, has been previously applied in the

comparison of different low-refractive index supporting materials for the enhancing Ag layer, as described in Ref. [36].

Glass slides were vapor-coated with Ag as described in the Experimental section (see above). This procedure is known to give Ag layers consisting of nanoparticles that are SERS-active. During storage and use, the SERS substrates were exposed to the normal laboratory atmosphere. Under these conditions, contaminant molecules can adhere to the Ag surface and subsequently decompose into carbonaceous material under laser irradiation. Using a  $20\times/\text{N.A.} = 0.7$  air objective, the beam of the 532-nm laser was focused onto the sample and spectra were recorded with an acquisition time of 1 s. All spectra presented in Fig. 4 were collected under these conditions.

The spectrum of an unprotected SERS substrate contains weak contributions from carbonaceous material, whose signal intensity grows significantly after 45 s of continuous laser irradiation (Fig. 4(a)). This again shows that carbonaceous material is generated during the experiment by photochemical or heat-induced decomposition of precursor molecules of unknown identity. Then, SERS slides were protected by immersion of freshly coated glass slides into  $10^{-3}\text{ M}$  methanolic EtSH solution for 5 min. This procedure is identical to the one described in the Experimental section for the protection of TERS tips. SERS spectra collected directly after protection and after 45 s of continuous laser irradiation are shown in Fig. 4(b). Directly after application of the protecting layer, only

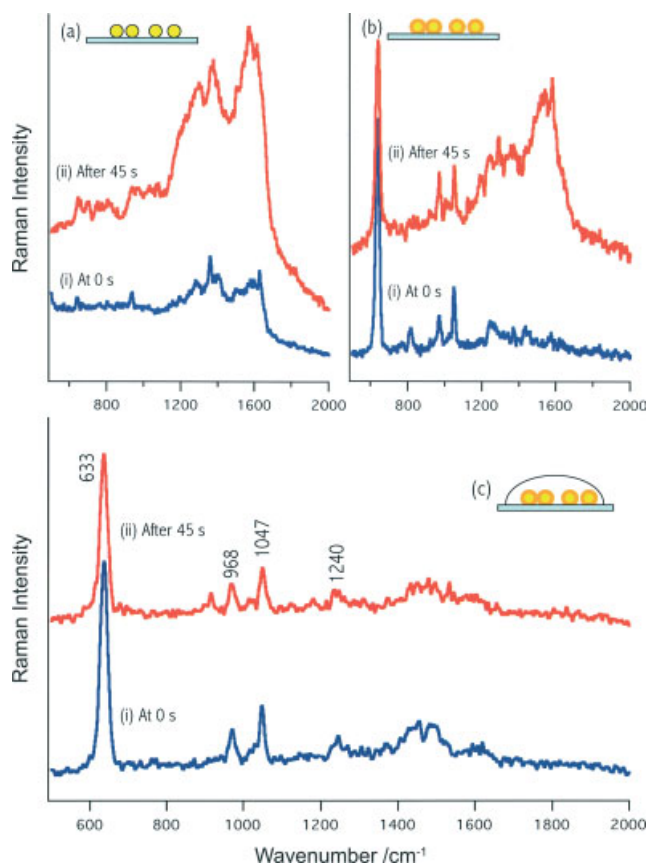


**Figure 4.** SERS measurements using unprotected and EtS-protected Ag substrates in air and in water: (a) spectra of an unprotected Ag slide taken (i) directly after vapor coating and (ii) after 45 s of continuous laser irradiation, (b) spectra of an EtS-protected SERS substrate collected in air, and (c) a different spot on the same SERS substrate measured in water. The collection time for each measurement was 1 s.

**Table 1.** Assignment of the most prominent vibrational modes of EtS

Vibrational assignment	SERS in water (this study) (cm <sup>-1</sup> )	SERS in air (Ref. [47]) (cm <sup>-1</sup> )
$\nu(\text{CS})$	633	632
$\delta(\text{CH})$	968	969
$\delta(\text{CH})$	1047	1047
$\beta(\text{CH})$	1240	1246

bands from EtS are detectable – with the most prominent band of EtS at 633 cm<sup>-1</sup> – and little or no contribution from carbonaceous material can be seen. This demonstrates that EtS is able to protect the Ag surface from carbon contamination. However, after laser illumination of the surface for 45 s, partial decomposition of EtS (or of other, unknown precursor molecules) into carbonaceous material was detected. Figure 4(c) represents a SERS experiment that simulates a protected TERS tip in an aqueous environment. Spectra of an EtS-protected SERS substrate with a droplet of water on top were collected under the same conditions. Both spectra, taken directly after protection and after 45 s of continuous laser illumination, show the same result: distinct EtS bands, but little or no signs of carbon contamination. This is a key finding of this work: performing SERS or TERS experiments in water can reduce interfering carbon contamination signals. This is discussed in detail below. Furthermore, water does not induce band shifts as shown in Table 1, where band assignments and literature data from SERS performed in air are given.

From these results we can conclude that an EtS SAM can efficiently protect the Ag surface from contamination with carbonaceous material or other precursor molecules. After long/intense laser irradiation, photodecomposition of the protection layer into carbon was observed. This effect can be prevented – or at least slowed down considerably – if the experiment is performed in water. This can have two reasons. First, water acts as a heat sink and can reduce sample damage due to laser heating. Since a tightly focused laser is used for excitation and locally enhanced due to absorption and field enhancement by the Ag nanoparticles, heating effects might play a role. Recently, enhancing nanoshells have even been proposed for thermal antitumor therapy.<sup>[48]</sup> Secondly, oxygen is known to play a significant role in the generation of carbonaceous contaminants and their fluctuating SERS spectra.<sup>[49]</sup> The solubility of molecular oxygen in water is only 7.6 mg l<sup>-1</sup> at 20 °C,<sup>[50,51]</sup> which corresponds to a molar fraction of 4.3 ppm. The volume fraction of oxygen in air is 20.95% (209 476 ppm),<sup>[51]</sup> which is equal to the molar fraction if we assume ideal gas behavior. Thus, compared to the amount of other molecules, there is approximately 50 000 times less oxygen available around the tip, if the experiment is performed in water.

As shown above, EtS-protected Ag surfaces have clear advantages compared to unprotected surfaces in terms of carbon contamination signals. To characterize the behavior of protected tips in a TERS experiment, we performed measurements of BCB dye in air. TERS of BCB is a standard experiment performed in several laboratories, which allows an easy comparison of the enhancement of different tips. In this case, our aim was to study the influence of EtS protection on the enhancement. Figure 5 shows spectra obtained with an unprotected tip in contact with a BCB sample (a), with an EtS-protected tip (b), and with the tip retracted (c). All measurements were performed under the same conditions, with a laser power of 2 μW at the sample and a collection time

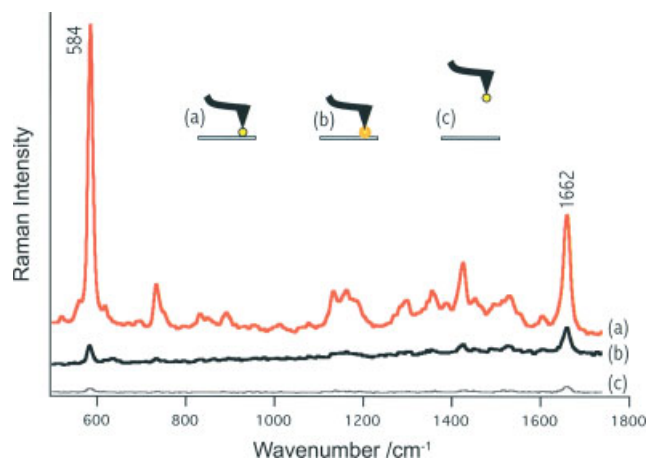


**Figure 5.** TER spectra of BCB collected in air demonstrating differences in enhancement between unprotected and EtS-protected tips: TER spectra collected with (a) an unprotected and (b) an EtS-protected tip in contact with a thin film of BCB on a glass slide, and (c) far-field spectrum corresponding to measurement (a). The collection time for each measurement was 10 s.

of 10 s. The BCB sample dominates the spectrum in all cases, i.e. EtS bands are obscured by the BCB Raman bands, due to an additional preresonance enhancement of BCB at the excitation laser wavelength used.

For comparison of TERS experiments with protected and unprotected tips, enhancement factors were calculated as described in Refs. [4, 27, and 36]. There are two parameters to gauge the enhancement by a TERS tip: the contrast and the enhancement factor. The contrast is the ratio between the intensities of near-field and far-field signal, whereas the enhancement factor additionally takes into account that the source of the near-field signal is much smaller than the one of the far-field signal. The enhancement factor is the contrast multiplied with the ratio of far-field and near-field volumes. In the case of thin film samples, such as spin-cast BCB on a glass substrate, the corresponding surface areas can be considered instead of the volumes.<sup>[4]</sup> In this study, the enhancement factor was calculated according to the following equation:

$$EF = \frac{I_{NF}}{I_{FF}} \frac{A_{FF}}{A_{NF}} = \frac{I_{\text{tip in}} - I_{\text{tip out}}}{I_{\text{tip out}}} \frac{A_{FF}}{A_{NF}} = \left( \frac{I_{\text{tip in}}}{I_{\text{tip out}}} - 1 \right) \frac{A_{FF}}{A_{NF}} = C \frac{A_{FF}}{A_{NF}} \quad (1)$$

where *EF* and *C* denote the enhancement factor and contrast, respectively. The indices NF and FF denote near field and far field, and *I* and *A* are the corresponding signal intensities and source areas, respectively. *I*<sub>tip in</sub> is the signal intensity measured with the tip in contact with the sample, and *I*<sub>tip out</sub> is the corresponding signal intensity detected with the tip retracted from the sample. For the estimates of the source areas, diameters of 500 nm for far field (approximate diameter of the laser focus) and 40 nm for near field were used in the calculation, values that have been used previously in similar studies with this experimental setup.<sup>[27,36,52]</sup> The estimate for the diameter of the near-field source area is a typical tip apex diameter obtained with our coating procedure.<sup>[36,52]</sup> It should be pointed out that the values of near-field diameter and enhancement factor are upper and lower limits, respectively, since earlier studies have shown that the lateral resolution of TERS with metal-coated tips is smaller than the tip apex.<sup>[53]</sup>

With unprotected tips, a contrast of  $\sim 60\times$  was achieved, corresponding to an enhancement factor of  $\sim 10^4$ . This is comparable to enhancements obtained with  $\text{AlF}_3/\text{Ag}$  tips.<sup>[36]</sup> The protection caused a decrease of the contrast by a factor of  $\sim 5$ , yielding an enhancement factor of  $\sim 10^3$ . This drop in enhancement is probably due to a combination of several effects: (1) the tip-sample distance is increased by the size of EtS, which is approximately 4.5 Å. This is much smaller than the extent of the enhanced field, but the field enhancement is the strongest at the tip's surface and drops rapidly with increasing distance from the tip.<sup>[7,46]</sup> (2) Direct contact between Ag and analyte is prevented, i.e. additional chemical enhancement is suppressed. (3) A shift of the surface plasmon resonance wavelength induced by the adsorbed protection material has to be considered. Compared to the spectrum enhanced by an unprotected tip, the band intensity at  $584\text{ cm}^{-1}$  drops significantly more than the one at  $1162\text{ cm}^{-1}$ , which indicates a red shift of the surface plasmon resonance, further away from the laser wavelength and thus leading to a reduced enhancement.

### Proof of principle: TERS of PhS on Au in water using protected tips

Finally, a proof-of-principle experiment with both the PhS sample and EtS-protected tip immersed in water was performed. When the tip was in contact with a PhS SAM on Au in water, a high signal-to-noise-ratio TER spectrum was collected within 10 s (Fig. 6(a)). Both background and Raman signals are elevated as compared to the far-field spectrum in Fig. 6(c). The increase in background signal intensity has been recently attributed to photons emitted from annihilated inelastically scattered localized surface plasmons.<sup>[54]</sup> The TER bands observed at 1576, 1073, 1023, 1000, and  $690\text{ cm}^{-1}$  can be clearly assigned to PhS (for assignments see Table 2). The wavenumbers agree well with the vibrational spectra of PhS on Au surfaces and Ag thiophenolate salts.<sup>[39]</sup> The contrast between near-field and far-field signal is approximately  $20\times$ , corresponding to an enhancement factor of  $\sim 3 \times 10^3$ .

After the TERS measurements, the Raman spectra of the tips themselves were acquired using a clean Au surface as substrate. Essentially, only EtS signals from the tip protection layer are left in the spectrum shown in Fig. 6(b) and only very weak PhS signals were observed. No carbon contamination was found. These findings are significant, as they show that the EtS adsorbs strongly to the tip. This renders the tip more inert towards contamination. The  $\nu(\text{CS})$  band of EtS at  $633\text{ cm}^{-1}$  appears with equal intensities on both the TER and control spectrum (Fig 6(a) and 6(b)). This is an important feature of our experiment, because this band serves as a check for the reproducibility of the laser beam alignment to the tip. If the laser beam is not well aligned, an under- or over-quantification of material adsorbed on the tip will result. Additionally, in mapping/imaging experiments planned for the future, this band can serve as an internal standard for normalization of signal intensities.

## Conclusions

We demonstrated for the first time TERS experiments performed in a liquid. Enhancement factors of  $>10^3$  have been achieved in water using  $\text{SiO}_x/\text{Ag}$ -coated tips, PhS SAMs on Au as a sample, and 532-nm excitation. Furthermore, we described strategies for fabrication of robust tips and their protection from contamination. The latter has been shown to reduce the enhancement. Thus,

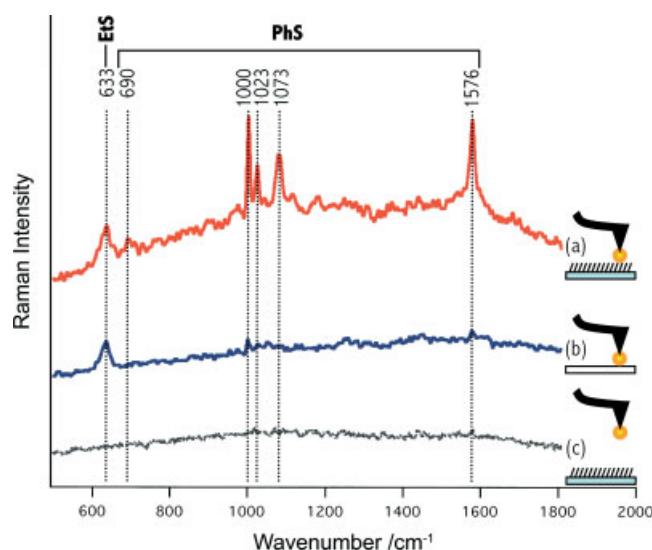


**Figure 6.** Proof-of-principle experiment demonstrating the feasibility of performing TERS in water using EtS-protected tips: (a) TER spectrum of a PhS SAM on Au collected in water, (b) control experiment performed after measurement (a) with the same tip in contact with a clean Au surface, and (c) far-field measurement corresponding to measurement (a). The collection time for each spectrum was 10 s.

**Table 2.** Assignment of the most prominent vibrational modes of PhS

Band assignments	SAM of PhS on Au surface		Raman spectrum of Ag-PhS (Ref. [39]) ( $\text{cm}^{-1}$ )
	TERS (this study) ( $\text{cm}^{-1}$ )	SERS (Ref. [39]) ( $\text{cm}^{-1}$ )	
$\nu(\text{CC})$	1576	1573	1574
$\beta(\text{CCC}) + \nu(\text{CS})$	1073	1073	1079
$\beta(\text{CH})$	1023	1022	1020
$\beta(\text{CCC})$	1000	999	998
$\beta(\text{CCC}) + \nu(\text{CS})$	690	691	694

we propose that the use of protected or unprotected tips should be decided depending on the sample under investigation, and whether tip contamination by analyte molecules plays a significant role or not. This study opens the door to the investigation of biological cells, cell membranes, or supported lipid bilayers in aqueous environments by TERS.

### Acknowledgements

This work has been supported by ETH Zurich. Grace Leong acknowledges Novartis for a M.Sc. scholarship and Johannes Stadler thanks the Roche Research Foundation for a Ph.D. scholarship. We would like to thank the Electron Microscopy Center at ETH Zurich (EMEZ), and Frank Krumeich for performing the SEM analyses.

### References

- [1] B. I. de Bakker, A. Bodnar, E. M. H. P. van Dijk, G. Vamosi, S. Damjanovich, T. A. Waldmann, N. F. van Hulst, A. Jenei, M. F. Garcia-Parajo, *J. Cell Sci.* **2008**, *121*, 627.

- [2] C. Hoppener, L. Novotny, *Nano Lett.* **2008**, *8*, 642.
- [3] M. L. Kraft, P. K. Weber, M. L. Longo, I. D. Hutcheon, S. G. Boxer, *Science* **2006**, *313*, 1948.
- [4] T. Schmid, B. S. Yeo, W. Zhang, R. Zenobi, in *Tip Enhancement: Advances in Nano-Optics and Nano-Photonics* (Eds.: S. Kawata, V. M. Shalaev), Elsevier B.V.: Amsterdam, **2007**, pp 115.
- [5] A. Hartschuh, N. Anderson, L. Novotny, *J. Microsc. Oxford* **2003**, *210*, 234.
- [6] N. Hayazawa, T. Yano, H. Watanabe, Y. Inouye, S. Kawata, *Chem. Phys. Lett.* **2003**, *376*, 174.
- [7] B. Pettinger, B. Ren, G. Picardi, R. Schuster, G. Ertl, *J. Raman Spectrosc.* **2005**, *36*, 541.
- [8] R. M. Stöckle, Y. D. Suh, V. Deckert, R. Zenobi, *Chem. Phys. Lett.* **2000**, *318*, 131.
- [9] M. S. Anderson, *Appl. Phys. Lett.* **2000**, *76*, 3130.
- [10] N. Hayazawa, Y. Inouye, Z. Sekkat, S. Kawata, *Opt. Commun.* **2000**, *183*, 333.
- [11] N. Hayazawa, Y. Inouye, Z. Sekkat, S. Kawata, *J. Chem. Phys.* **2002**, *117*, 1296.
- [12] N. Hayazawa, A. Tarun, Y. Inouye, S. Kawata, *J. Appl. Phys.* **2002**, *92*, 6983.
- [13] B. Pettinger, B. Ren, G. Picardi, R. Schuster, G. Ertl, *Phys. Rev. Lett.* **2004**, *92*, 096 101.
- [14] D. L. Stokes, Z. H. Chi, T. Vo-Dinh, *Appl. Spectrosc.* **2004**, *58*, 292.
- [15] C. C. Neacsu, J. Dreyer, N. Behr, M. B. Raschke, *Phys. Rev. B* **2006**, *73*, 193 406.
- [16] K. F. Domke, D. Zhang, B. Pettinger, *J. Am. Chem. Soc.* **2006**, *128*, 14 721.
- [17] W. H. Zhang, B. S. Yeo, T. Schmid, R. Zenobi, *J. Phys. Chem. C* **2007**, *111*, 1733.
- [18] J. Steidtner, B. Pettinger, *Phys. Rev. Lett.* **2008**, *100*, 236 101.
- [19] N. Anderson, P. Anger, A. Hartschuh, L. Novotny, *Nano Lett.* **2006**, *6*, 744.
- [20] N. Anderson, A. Bouhelier, L. Novotny, *J. Opt. A Pure Appl. Op.* **2006**, *8*, S227.
- [21] N. Anderson, A. Hartschuh, S. Cronin, L. Novotny, *J. Am. Chem. Soc.* **2005**, *127*, 2533.
- [22] N. Anderson, A. Hartschuh, L. Novotny, *Nano Lett.* **2007**, *7*, 577.
- [23] A. Hartschuh, H. H. Qian, A. J. Meixner, N. Anderson, L. Novotny, *Nano Lett.* **2005**, *5*, 2310.
- [24] T. A. Yano, Y. Inouye, S. Kawata, *Nano Lett.* **2006**, *6*, 1269.
- [25] H. Watanabe, Y. Ishida, N. Hayazawa, Y. Inouye, S. Kawata, *Phys. Rev. B* **2004**, *69*, 155 418.
- [26] N. Hayazawa, H. Watanabe, Y. Saito, S. Kawata, *J. Chem. Phys.* **2006**, *125*, 244 705.
- [27] T. Schmid, A. Messmer, B. S. Yeo, W. H. Zhang, R. Zenobi, *Anal. Bioanal. Chem.* **2008**, *391*, 1907.
- [28] T. Schmid, J. Burkhard, B. S. Yeo, W. H. Zhang, R. Zenobi, *Anal. Bioanal. Chem.* **2008**, *391*, 1899.
- [29] B. S. Yeo, S. Madler, T. Schmid, W. H. Zhang, R. Zenobi, *J. Phys. Chem. C* **2008**, *112*, 4867.
- [30] E. Bailo, V. Deckert, *Angew. Chem. Int. Ed.* **2008**, *47*, 1658.
- [31] U. Neugebauer, P. Rosch, M. Schmitt, J. Popp, C. Julien, A. Rasmussen, C. Budich, V. Deckert, *ChemPhysChem* **2006**, *7*, 1428.
- [32] U. Neugebauer, U. Schmid, K. Baumann, W. Ziebuhr, S. Kozitskaya, V. Deckert, M. Schmitt, J. Popp, *ChemPhysChem* **2007**, *8*, 124.
- [33] M. De Serio, A. N. Bader, M. Heule, R. Zenobi, V. Deckert, *Chem. Phys. Lett.* **2003**, *380*, 47.
- [34] M. De Serio, H. Mohapatra, R. Zenobi, V. Deckert, *Chem. Phys. Lett.* **2006**, *417*, 452.
- [35] C. Vannier, B. S. Yeo, J. E. Melanson, R. Zenobi, *Rev. Sci. Instrum.* **2006**, *77*, 023 104.
- [36] B. S. Yeo, T. Schmid, W. Zhang, R. Zenobi, *Anal. Bioanal. Chem.* **2007**, *387*, 2655.
- [37] X. D. Cui, W. H. Zhang, B. S. Yeo, R. Zenobi, C. Hafner, D. Erni, *Opt. Express* **2007**, *15*, 8309.
- [38] K. T. Carron, L. G. Hurlley, *J. Phys. Chem.* **1991**, *95*, 9979.
- [39] T. H. Joo, M. S. Kim, K. Kim, *J. Raman Spectrosc.* **1987**, *18*, 57.
- [40] J. A. Dieringer, A. D. McFarland, N. C. Shah, D. A. Stuart, A. V. Whitney, C. R. Yonzon, M. A. Young, X. Y. Zhang, R. P. Van Duyne, *Faraday Discuss.* **2006**, *132*, 9.
- [41] B. Ren, G. Picardi, B. Pettinger, R. Schuster, G. Ertl, *Angew. Chem. Int. Ed.* **2005**, *44*, 139.
- [42] T. Deckert-Gaudig, E. Bailo, V. Deckert, *J. Biophoton.* **2008**, *1*, 377.
- [43] K. F. Domke, D. Zhang, B. Pettinger, *J. Phys. Chem. C* **2007**, *111*, 8611.
- [44] D. Mehtani, N. Lee, R. D. Hartschuh, A. Kisliuk, M. D. Foster, A. P. Sokolov, J. F. Maguire, *J. Raman Spectrosc.* **2005**, *36*, 1068.
- [45] A. Hartschuh, E. J. Sanchez, X. S. Xie, L. Novotny, *Phys. Rev. Lett.* **2003**, *90*, 095 503.
- [46] A. Downes, D. Salter, A. Elfick, *J. Phys. Chem. B* **2006**, *110*, 6692.
- [47] C. H. Kwon, D. W. Boo, H. J. Hwang, M. S. Kim, *J. Phys. Chem. B* **1999**, *103*, 9610.
- [48] S. Lal, S. E. Clare, N. J. Halas, *Accounts Chem. Res.* **2008**, *41*, 1842.
- [49] A. Kudelski, *J. Phys. Chem. B* **2006**, *110*, 12610.
- [50] J. Emsley, *Nature's Building Blocks*, Oxford University Press: Oxford, **2003**.
- [51] D. R. Lide, *Handbook of Chemistry and Physics*, CRC Press: Boca Raton, **2008**.
- [52] B. S. Yeo, W. Zhang, C. Vannier, R. Zenobi, *Appl. Spectrosc.* **2006**, *60*, 1142.
- [53] J. J. Wang, Y. Saito, D. N. Batchelder, J. Kirkham, C. Robinson, D. A. Smith, *Appl. Phys. Lett.* **2005**, *86*, 263 111.
- [54] B. Pettinger, K. F. Domke, D. Zhang, R. Schuster, G. Ertl, *Phys. Rev. B* **2007**, *76*, 113 409.